STUDIA UBB CHEMIA, LVII, 3, 2012 (p. 213 – 222)
(RECOMMENDED CITATION)

A COMPUTATIONAL STUDY OF THE SURFACE PROPERTIES OF THE HUMAN AND BACTERIAL CHITOTRIOSIDASE

ALECU-AUREL CIORSAC[1], VASILE OSTAFE[2, 3], ADRIANA ISVORAN[2, 3]

ABSTRACT. Mapping of physicochemical properties of surfaces of the human, bacterial and fungal chitotriosidases reveals that the three enzymes present distinct local surface properties, suggesting the possibility of specific inhibition of the human chitotriosidase. The results obtained for the volumes of the largest cavity differ qualitatively and quantitatively between the two employed tools (CASTp and Fpocket). Nevertheless, both algorithms concur in indicating that the human, bacterial and fungal chitotriosidase pockets are different.

Keywords: *chitotriosidase, fractal surface dimension, surface properties, ligand binding, specific inhibition.*

INTRODUCTION

Chitinases belong to the glycosyl hydrolase 18 family that cleave the glycosidic bond in chitin, and are found in bacteria, fungi, insects, plants and mammals [1]. Although it was thought for many years that humans do not possess and process chitin, it was more recently discovered that humans have a chitinase activity associated to conditions such as allergies, asthma, fungal infections and cancer [2]. Among the human chitinases, chitotriosidase (CHT) and acidic mammalian chitinase (AMCase) hydrolise the chitin [3] contained in fungal cell walls and exoskeletons of numerous parasitic worms [4]. Even if the biological function of CHT is not yet fully established, it is already known that it plays an important role as a pathogen-defence protein. Chitotriosidase is a specific marker for lysozomal storage disorders and it was also proposed to be a possible target for the design of chemotherapeutics against human pathogens [1, 5] [7]. Most chitotriosidase inhibitors show no selectivity and competitively inhibit family 18 chitinases [8, 9]. It becomes important to identify common inhibitors of human CHT, family 18 chitinases and chitinases in the pathogenic organisms and to design new specific inhibitors for CHT.

[1] *Politehnica University of Timisoara, Department of Physical Education and Sport, 2 P-ta Victoriei, RO-300006, Timisoara, Romania*
[2] *West University of Timisoara, Department of Chemistry, 16 Pestallozi, RO-300115, Timisoara, Romania, aisvoran@cbg.uvt.ro*
[3] *Laboratory of Advanced Researches in Environmental Protection, 4 Oituz, Timisoara, RO-300086, Romania*

Here, we analyze the surface properties of the human bacterial and fungal chitotriosidases in correlation with those of their known ligands, in order to obtained clues useful for the design of new possible therapeutic molecules selectively blocking the human CHT enzymatic activity.

RESULTS AND DISCUSSION

The sequences of the human, fungal (*Aspergillus fumigatus*) and bacterial (*Serratia marcescens*) chitotriosidases, retrieved from UniProtKB databases (codes entry Q13213, Q54276 and Q873X9 respectively), reveal only 48% sequence identity (data not shown).

Figure 1 illustrates the determination of the surface fractal dimension for the free human chitotriosidase. The computed fractal dimension is 2.24±0.01 and it reflects the complexity of the surface shape of the protein in good agreement with other published data concerning fractal aspects of protein surfaces [10-12].

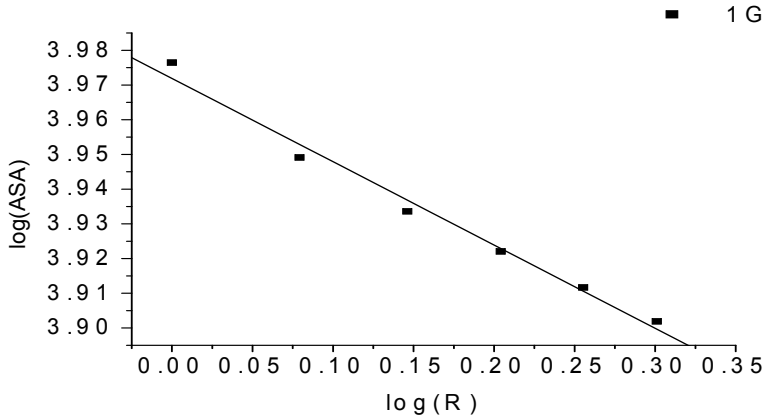

Figure 1. Determination of the global fractal dimension of human chitotriosidase (pdb entry 1GUV)

The surface fractal dimensions for the surfaces corresponding to all the considered chitotrisidases determined using this algorithm are presented in Table I, alongside the root mean square deviation (RMSD) obtained by superimpositions of the structure of human chitotriosidase and the other considered structures.

The superimposition of structural files indicates that globally the structural properties of the investigated CHTs are relatively similar. Thus, between the bacterial and fungalCHTs the RMSD values are situated around 0.828 Å. Between the human CHT and its complexes there are only small differences, and this is also true for *Serratia marcescens* (RMSD between 0.345 Å and 0.398 Å) and *Aspergillus fumigatus* (RMSD between 0.346 Å and 0.562 Å). The

accessible surface area is higher for the free CHT in comparison to that of its complexes, and the surface fractal dimension is smaller for the free CHT. These results emphasise the high complexity of the protein surface and its sensitive conformational changes when the protein interacts with ligands.

Table I. Global surface properties for considered chitotriosidases and their complexes (ASA – accessible surface area; Df – fractal dimension, electrostatics-based 'contact potential'). The ligand was removed from the structural file when computing the surface properties of the complexed proteins.

Chitotriosidase	PDB code	RMSD (Å)	ASA (Å^2)	D_f	Contact potential
Human CHT free	1GUV	-	8894.94	2.24±0.01	-57.68 +57.68
Human CHT in complex with chitobiose	1LG1	0.439	8405.06	2.30±0.02	-58.02 +58.02
Human CHT in complex with ethylene glycol	1LG2	0.495	8120.77	2.31±0.01	-57.64 +57.64
Human CHT in complex with glucoallosamidin B	1HKI	0.361	8366.75	2.28±0.02	-57.90 +57.90
Human CHT in complex with methylallosamidin	1HKJ	0.370	8322.26	2.34±0.02	-56.41 +56.41
Human CHT in complex with allosamidin	1HKK	0.413	8230.84	2.28±0.02	-58.07 +58.07
Human CHT in complex with demethylallosamidin	1HKM	0.373	8249.76	2.27±0.03	-57.24 +57.24
Human CHT in complex with argadin	1WAW	0.528	8282.47	2.30±0.01	-56.98 +56.98
Human CHT in complex with argifin	1WB0	0.429	8373.07	2.27±0.02	-57.09 +57.09
Serratia marcescens CHT	1E15	1.108	7785.90	2.20±0.02	-48.41 +48.41
D142N mutant of serratia marcescens CHT in complex with allosamidin	1OGG	1.014	7725.90	2.11±0.02	-47.81 +47.81
Aspergillus fumigatus CHT	1W9P	1.129	8893.97	2.26±0.03	-55.03 +55.03
Aspergillus fumigatus CHT in complex with argadin	1W9U	1.116	9029.36	2.25±0.02	-55.01 +55.01
Aspergillus fumigatus CHT in complex with argifin	1W9V	1.112	8956.74	2.24±0.03	-55.06 +55.06
Aspergillus fumigatus CHT in complex with theofillin	2A3A	1.102	9168.12	2.24±0.02	-55.02 +55.02
Aspergillus fumigatus CHT in complex with caffeine	2A3B	1.117	9171.72	2.25±0.02	-55.12 +55.12
Aspergillus fumigatus CHT in complex with pentoxifillin	2A3C	1.111	9169.94	2.24±0.01	-55.09 +55.09
Aspergillus fumigatus CHT in complex with alosamidin	2A3E	0.996	9156,89	2.22±0.02	-55.27 +55.27

Table I also shows differences between the structures and surfaces of bacterial, fungal and human chitotriosidases, which are in line with the sequence dissimilarities. Contact potential calculations reveal that local charge density is different for the three CHTs. This property, in addition to other determined surface properties of the investigated proteins and the structural features of ligands, allows us to predict possible regions for charged ligands binding. Also, the solvent accessible surface is higher for fungal CHTs in comparison with human and bacterial CHTs. We must underline that human CHT is a monomer and bacterial and fungal CHTs form dimers.

The dimensional properties of the largest cavity identified for the chitotrisidases using the CASTp [13] software are presented in Table II, and help to assess the accessibility of this cavity to various ligands and substrates. Additionally, the Fpocket [14] data in Table II also reveal that the largest identified pockets for all considered chitotriosidases usually have hydrophobic character and present local regions of high hydrophobic density.

The volumes of the pockets are different when identified by CASTp and Fpocket. Disturbingly, the differences are on the order of 100-200%, and no trends are conserved. Whereas CASTp claims that the bacterial enzyme has the largest pocket (almost three times larger than human and fungi CHTs), Fpocket claims that the bacterial enzyme has smaller pocket, almost half of one of the pockets seen in one of the human enzymes. Nevertheless, both algorithms concur in saying that the human, fungal and bacterial pockets are different. Unavoidably, the scoring functions are strongly dependent on the quality of the pocket identification and delimitation and they are sensitive to conformational changes. All these reflect that both of two servers give the probable but not exact binding pockets and makes comparison between methods difficult and only qualitative in nature. It has been also proved that the pocket volume computed by Fpocket is only approximated [14]. On the other hand the advantage of Fpocket is that it also specifies the global and local hydrophobicity, important for ligand binding. The values presented in Table II also emphasise that the structural changes that occur when CHT interacts with its ligands strongly affect the surface properties. These changes may be understood easier if we take into account also the properties of the ligands (as computed using the chimera software [15]), cf. Table III. The volumes and surface areas of known CHT ligands are smaller in comparison to those identified for the cavities by the CASTp software.

Figure 2 illustrates the largest pocket identified for CHT using the Fpocket tool. The pocket is presented as grey small spheres and the protein is presented as cartoon.

Table II. Geometrical properties of the biggest cavity identified by CASTp and Fpocket respectively into the investigated structures

Chitotrisodase/ Chitotriosidase complex	PDB code entry	CASTp		Fpocket		
		Area (Å^2)	Volume (Å^3)	Hydrophobicity score	Local hydrophobic density	Pocket volume (Å3)
Human CHT free	1GUV	823.6	1518.5	31.28	53.49	2207.92
Human CHT in complex with chitobiose	1LG1	821.1	1371.4	30.66	45.92	2634.06
Human CHT in complex with ethylene glycol	1LG2	749.0	1264.2	28.46	45.44	1869.06
Human CHT in complex with glucoallosamidin B	1HKI	829.1	1353.6	27.02	47.98	1832.71
Human CHT in complex with methylallosamidin	1HKJ	821.8	1397.6	35.28	48.98	2530.02
Human CHT in complex with allosamidin	1HKK	749.1	1305.0	32.51	54.45	2461.55
Human CHT in complex with demethylallosamidin	1HKM	842.5	1406.5	34.71	52.68	1863.28
Human CHT in complex with argadin	1WAW	894.8	1630.1	31.07	57.98	3107.77
Human CHT in complex with argifin	1WB0	782.1	1322.9	18.77	33.05	1144.65
Serratia marcescens CHT	1E15	1929.0	3506.1	24.38	57.52	1716.32
D142N mutant of Serratia marcescens CHT in complex with allosamidin	1OGG	1848.6	3686.1	27.76	54.39	1842.65
Aspergillus fumigatus CHT	1W9P	686.7	981.1	26.90	47.25	1931.73
Aspergillus fumigatus CHT in complex with argadin	1W9U	826.6	1402.4	26.63	46.74	1811.49
Aspergillus fumigatus CHT in complex with argifin	1W9V	817.6	1384.8	30.22	37.25	1481.11
Aspergillus fumigatus CHT in complex with theofillin	2A3A	768.7	1271.4	27.00	45.37	1484.51
Aspergillus fumigatus CHT in complex with caffeine	2A3B	851.7	1315.2	22.09	39.18	1100.90
Aspergillus fumigatus CHT in complex with pentoxifillin	2A3C	1165.2	1854.9	18.99	58.68	690.32
Aspergillus fumigatus CHT in complex with alosamidin	2A3E	856.8	1350.6	22.87	37.29	724.44

Table III. Geometrical properties of known ligands

Ligand	Surface area (Å^2)	Volume (Å^3)
chitobiose	322.8	339.5
ethylene glycol	341.2	281.3
glucoallosamidin B	484.1	533.2
methylallosamidin	498.1	556.8
allosamidin	933.4	1106
demethylallosamidin	462.7	505.1
argadin	904.5	954.1
argifin	976.3	919.0

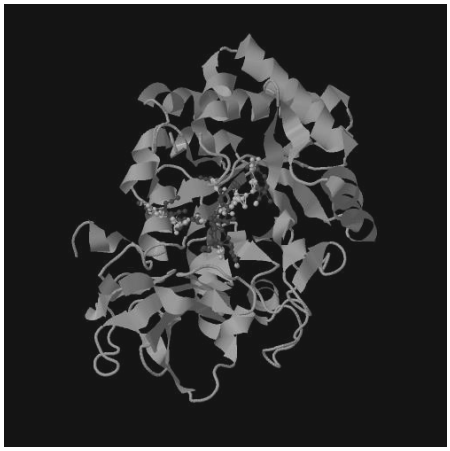

Figure 2. The largest pocket (grey spheres) for the human chitotriosidase (code entry 1GUV) detected using Fpocket

CONCLUSIONS

Mapping of physicochemical characteristics onto the surface of a protein can be used in the characterization and identification of similarities within protein surface regions. We have used this mapping to compare the surface properties of human, bacterial and fungal chitotriosidases. Our study reveals distinct surface properties for human, bacterial and fungi CHTs and also underlines that interactions of protein with its ligands affect the surface properties, such as solvent accessible area and surface roughness.

There are a few determined three dimensional structures of the human chitotriosidase in complex with inhibitors such as chitooligossacharide [1], allosamin and its derivatives, demethylallosamidin, methylallosamidin, and glucoallosamidin B [17] and two natural peptide products, argifin and argadin [18]. These structures show that the effect of inhibition is the alteration of the hydrophobic interactions and hydrogen binding [1, 17, 18]. Our data, predicting a large hydrophobic binding pocket in the structures of investigated CHTs, are in good agreement with these findings revealing an elongated active site cleft compatible with the binding of chitinopolymers. Also, our data suggest that the active site has an open architecture and a potential selective inhibitor of CHT must be a hydrophobic molecule.

The sequence differences and structural dissimilarities of the bacterial, fungal and human chitotriosidases reflected in their distinct surface properties allow us to speculate that there is the possibility of designing specific inhibitors for human chitotriosidases.

EXPERIMENTAL SECTION

For the human and bacterial chitotriosidase (CHT) the surface properties examined within this study are: the solvent accessible area (ASA) of the protein, the surface roughness, the dimensional and physicochemical properties of its identified cavities and/or pockets and its electric potential respectively. The three dimensional structures of free CHT and of its complexes with small drug molecules are retrieved from the Protein Data Bank [19] and their entry codes are presented in Table 1. When more than one chain is present in the structural file (as in the case of bacterial CHT), only one monomer (chain A) is considered.

The protein surface area can be computed starting from various models[20]. For example, in order to identify the protein surface cavities the CASTp [13] or Fpocket [15] tools may be used, and in order to compute the accessible surface area the GETAREA [21] tool may be used. CASTp provides identification and measurements of surface accessible pockets as well as interior inaccessible cavities using the weighted Delaunay triangulation and the alpha complex for shape measurements [13]. It computes a triangulation of the protein's surface atoms using alpha shapes and these triangles are then grouped by letting small triangles flow toward neighbouring larger triangles, which act as sinks. The pocket is defined as the collection of empty triangles. The Fpocket detection algorithm is based on Voronoi tessellation and also allows to extract pocket descriptors and a druggability prediction score [14]. This tool is based on the geometric approach of an alpha sphere contacting four atoms on its boundary (all the four atoms are at an equal distance, sphere

radius, to the alpha sphere centre) and containing no internal atom. Alpha sphere identification is based on Voronoi decomposition of space: the centre of alpha spheres correspond to Voronoi vertices, i.e. points at which Voronoi regions intersect. Next step consists in identifying clusters of spheres close together, to identify pockets, and to remove clusters of poor interest. For proteins, small spheres are located within the protein, clefts and cavities correspond to spheres of intermediate radii and large spheres are located at the protein surface. It is then possible to filter the ensemble of alpha spheres according to some minimal and maximal radii values in order to address pocket detection. After that the properties of the atoms of the pocket are considered in order to score each pocket.

In our study we have considered only the largest identified pocket as such a pocket tends to frequently correspond to the observed ligand binding site [21].

Another property that we investigate is the surface roughness quantitatively expressed by the surface fractal dimension. In order to determine this quantity we compute the surface area SA of each protein for different radii of the rolling probe using the on-line tool GETAREA [22] . The surface fractal dimension is determined using the scaling law between the surface area *(SA)* of the protein and the radius of the rolling probe molecule *(R)*

$$SA \sim R^{2-D_s} \tag{1}$$

from the slope of the double logarithmical plot of *SA* versus *R* [23]. The surface area of the protein has been calculated using the probe radii of 1, 1.2, 1.4, 1.6, 1.8 and 2 Å respectively.

The qualitative electrostatic properties of the surfaces of investigated structures, expressed by the contact potential, are computed using the PyMol software [16]. This software can provide information on the local charge density (within 10 angstroms), regarding how positive, negative or neutral a region of the protein surface is relative to the rest of the protein.

ACKNOWLEDGMENTS

This study benefited by the financial support of projects POSDDRU 21/1.5/G/38347, IPA-464 ROSNET and POSDRU 21/1.5/13798.

REFERENCES

1. F. Fusetti, H. von Moeller, D. Houston, H.J. Rozeboom, B.W. Dijkstra, R.G. Boot, J.M.F.G. Aerts, D.M.F. van Aalten, *Journal of Biological Chemistry,* **2002**, *27,* 25537.
2. J. Kzhyshkowska, A. Gratcev, S. Goerdt, *Biomarker Insights*, **2007**, *2*, 128.
3. G.H. Renkema, R.G. Boot, F.L. Au, *European Journal of Biochemistry*, **1998**, *251*, 504.
4. R.N. Tharanathan, F.S. Kittur, *Critical Reviews of Food and Scientific Nutrition*, **2003**, *43*, 61.
5. K.B. Eide, A.L. Norberg, E.B. Heggset, A.R. Lindbom, K.M. Vaarum, V.G.H. Eijsink, M. Sorlie, *Biochemistry*, **2012**, *51*, 487.
6. I.M.A. Nooren, J.M. Thornton, *EMBO Journal*, **2003**, *22*, 3486.
7. M. Kuepper, K. Bratke, J.C. Virchow, *Journal of Medicine,* **2008**, *358*, 1073.
8. C.L. Rush, A.W. Schuttelkopf, A.W. Hurtado-Guerrero, D.E. Blair, A.F.M. Ibrahim, D.S. Desvergnes, I.M. Eggleston, D.M. van Aalten, *Chemistry & Biology,* **2010**, *17*, 1275.
9. T.E. Sutherland, O.A. Andersen, M. Betou, I.M. Eggleston, R.M. Maizels, D.M. van Aalten, J.E. Allen, *Chemistry & Biology,* **2011**, *18*, 569.
10. A. Isvoran, *Chaos Solitons & Fractals*, **2004**, *19*, 141.
11. L. Pitulice, A. Isvoran, A. Chiriac, *Journal of the Serbian Chemical Society*, **2008**, *73,* 805.
12. A. Isvoran, L. Pitulice, C.T. Craescu, A. Chiriac, *Chaos Solitons & Fractals*, **2008**, *35*, 960.
13. J. Dundas, Z. Quyang, J. Tseng, A. Binkowski, Y. Turpaz, J. Liang, *Nucleic Acids Research,* **2006**, *34*, W116.
14. V. le Guilloux, P. Schmidtke, P. Tuffery, *BMC Bioinformatics,* **2009***, 10*, 168.
15. E.F. Pettersen, T.D. Goddard, C.C. Huang, G.S. Couch, D.M. Greenblatt, E.C. Meng, T.E. Ferrin, *Journal of Computational Chemistry*, **2004**, *25*, 1605.
16. W.L. DeLano, "The PyMOL Molecular Graphics System", DeLano Scientific, San Carlos, **2002**.
17. F.V. Rao, D.R. Houston, R.G. Boot, J.M. Aerts, S. Sakuda, D.M. van Aalten, *Journal of Biological Chem*istry, **2003**, *278*, 20110.
18. F.V. Rao, D.R. Houston, R.G. Boot, J.M. Aerts, M. Hodgkinson, D.J. Adams, S. Omura, D.M. van Aalten, *Chemical Biol*ogy, **2005**, *12*, 65.
19. H.M. Berman, J. Westbrook, Z. Feng, G. Gilliland, T.N. Bhat, H. Weissig, I.N. Shindyalov, P.E. Bourne, *Nucleic Acids Research,* **2000**, *28,* 235.

20. D. Crăciun, L. Pitulice, A. Isvoran, *International Journal of Chemical Modeling,* **2009**, *2*, 34.

21. M. Nayal, B. Honig, *Proteins: Structure, Function and Bioinformatics*, **2006**, *6,* 892.

21. R. Franczkiewicz, W. Braun, *Journal of Computational Chem*istry, **1998**, *19*, 319.

22. B.B. Mandelbrot, "Fractals and chaos. The Mandelbrot set and beyond", Springer Verlag, New York, **2004**, chapter 5.